

Characterization of PECVD grown porous SiO₂ thin films with potential application in an uncooled infrared detector

Pei-zhi Yang^{1,3}, Li-ming Liu², Jing-hui Mo² and Wen Yang¹

¹ Key laboratory of advanced renewable energy materials and fabrication technology, Ministry of education, Yunnan Normal University, Kunming 650092, People's Republic of China

² Kunming Institute of Physics, Kunming 650223, People's Republic of China

³ Institute of Solar Energy, Yunnan Normal University, Kunming 650092, People's Republic of China

E-mail: pzhyang@hotmail.com

Received 21 August 2009, in final form 21 December 2009

Published 9 March 2010

Online at stacks.iop.org/SST/25/045017

Abstract

Plasma-enhanced chemical vapor deposition (PECVD) technology was considered as an excellent thin film deposition dry process in semiconductor device fabrication. Porous SiO₂ film as a promising thermal insulation layer used in uncooled infrared detectors was grown directly by PECVD technology. The microstructure and elemental composition of the film were characterized by AFM, EDS, SEM and XPS. The porosity of the film was assessed according to the refractive index measured by ellipsometry. A prototype pyroelectric uncooled detector coated with a porous SiO₂ film was evaluated.

(Some figures in this article are in colour only in the electronic version)

Introduction

The thermal insulation structure plays a crucial role in uncooled infrared detectors such as pyroelectric detectors and microbolometers because it directly determines the thermal response [1–3]. In the early stage of uncooled infrared detectors development, multilayer film thermal isolation with a low thermal conducting structure was proposed. Based on this idea, a low thermally conducting porous SiO₂ film was sandwiched between the thermally sensitive layer and the Si substrate [4, 5]. Devices with such a structure can be easily fabricated by simple planarization semiconductor technology, and the mechanical strength can also be improved. Therefore, the isolation structure with a porous SiO₂ thin film possesses many advantages in practical application. Moreover, this isolation structure is quite suitable for property evaluation of thermally sensitive materials, and facilitates their integration into small-scale uncooled infrared detectors. To further improve the performance of thermal isolation, porous SiO₂ films with higher porosity and larger thickness are required [6].

Porous SiO₂ coatings are commonly prepared by sol–gel deposition [7, 8]. However, this is a wet chemical process, and post-heat treatment at a high temperature is unavoidable. Consequently, the sol–gel technique is not compatible with device fabrication processes. In comparison, plasma-enhanced chemical vapor deposition (PECVD) provides a novel approach for depositing thin films at a low temperature with a high deposition rate. In particular, PECVD is a dry procedure and circumvents the shortcomings (post-annealing treatment) of the sol–gel method [9]. Generally, there are two main approaches to produce porous oxide films by PECVD. The first one consists in the use of a polymeric sacrificial layer that is removed during deposition of the oxide thin film, and the second one relies on the modification of some critical deposition parameters [10]. Barranco *et al* used the first approach to grow porous SiO₂ films for antireflective coatings of photovoltaic modules [11].

In this study, we focused on the experimental study of the fabrication of porous SiO₂ film by PECVD using the second method, i.e. optimized process parameters. We proposed a novel and yet practical approach for producing a high-quality

Table 1. Deposition parameters of the porous SiO₂ films.

Working pressure (Torr)	0.9
RF power (W)	150
Inter-electrode distance (cm)	2
Substrate temperature (°C)	25
SiH ₄ +Ar gas mixture flow (sccm)	30
N ₂ O flow (sccm)	30
Deposition time (s)	1000

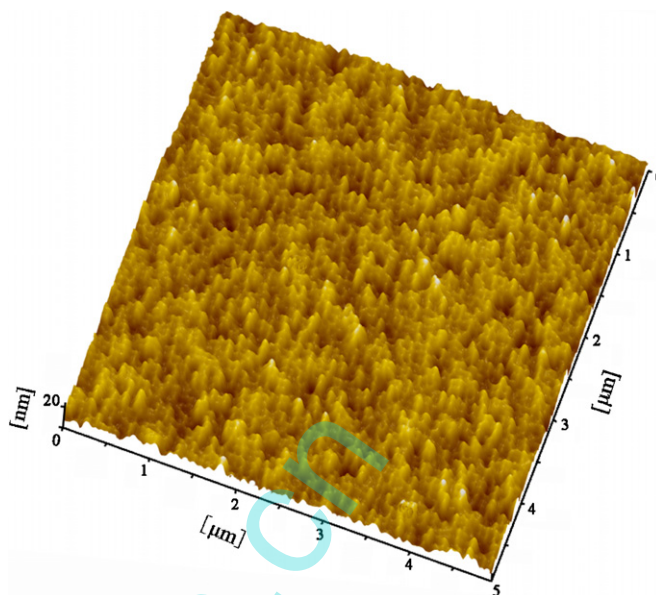
detector-grade porous SiO₂ film. Our results strongly support the idea that the porous SiO₂ film produced by PECVD using optimized process parameters can meet the requirements of uncooled infrared detectors.

Experiments

The porous SiO₂ films were deposited in a PECVD system (PECVD-2D type, Beijing Chuangweina Science and Technology Ltd, China) with a base pressure around 10⁻⁷ Torr. In the reactor, there are two parallel electrodes: the upper electrode (30 cm in diameter) is connected to an RF (13.56 MHz) power generator while the bottom one is the grounded electrode (30 cm in diameter), also functioning as the substrate holder. The sliding arrangement for the electrodes has been designed for inter-electrode spacing adjustment. The constant temperature circulation of water provided at the bottom electrode serves the purpose of maintaining a steady substrate temperature.

A P-type Si (1 0 0) wafer was used as the substrate. Prior to the deposition, the wafer was cleaned. Firstly, it was soaked in a H₂SO₄:H₂O₂=3:1 (Vol.) solution for 10 min and then rinsed with deionized (DI) water. Subsequently the wafer was etched in a HF:H₂O=1:9 (Vol.) solution for 1 min and then sprayed with DI water and dried with highly pure nitrogen gas. Argon (Ar) diluted silane (SiH₄) (10% SiH₄ + 90% Ar) and nitrous oxide (N₂O) were used as gaseous reactants. In our early works, it was found that the higher RF power, shorter inter-electrode distance and lower substrate temperature are three key factors for porous SiO₂ film deposition. In addition, the higher ratio of N₂O flow to SiH₄ flow is easy to produce the stoichiometric SiO₂ thin film (not non-stoichiometric SiO_x film). The working pressure (~0.9 Torr) used in our experiment is an appropriate value for plasma glow discharge. To obtain porous SiO₂ films with high quality, all these process parameters need to be carefully optimized. In this study, we used the approximately optimized process parameters (listed in table 1).

The thickness was monitored by an Ambios Technology XP-2 surface profilometer. The surface morphology and roughness were investigated using an atomic force microscope (AFM, CSPM 4000, Ben Yuan Ltd, China) operated in tapping mode. The elemental analysis of the film was performed by using energy-dispersive spectra (EDS) and x-ray photoelectron spectroscopy (XPS). The EDS analysis was obtained in a Philips XL30 ESEM-FEG system equipped with an EDAX light element detector. XPS was investigated on a photoelectron spectrometer (ESCA Lab 220i-XL) using Mg K α radiation as the exciting source. The refractive index of the

**Figure 1.** AFM image of the porous SiO₂ film.**Table 2.** Elemental composition of the porous SiO₂ film.

Element	Wt%	At%
O K	53.31	66.72
Si K	46.69	33.28

film was measured with an ellipsometer (Jobin Yvon HR460). To observe the pore structure of the films, high-resolution SEM images were obtained on the Philips XL30 ESEM-FEG system using an acceleration voltage of 30.0 kV.

Results and discussions

The thickness of the porous SiO₂ film measured by XP-2 was 1350 nm. Considering the deposition time (1000 s) of the film, the deposition speed could be calculated. The deposition rate was 13.5 Å s⁻¹ which is much higher than the usual deposition rate (about 5 Å s⁻¹) of dense SiO₂ thin films by our PECVD system. It is believed that the high growth rate helps to prepare porous SiO₂ thin films. By using high deposition rate, SiO₂ films of micron magnitude thickness can be obtained easily. The film thickness desired can be achieved by control of the deposition time.

Figure 1 shows an AFM image of the SiO₂ film prepared in this work. It is clear that the film exhibits a loose porous microstructure. The pore sizes of the film are in the range of a few hundred nanometers. The root-mean-square (RMS) surface roughness is about 6.5 nm.

Figure 2 shows the EDS spectrum of the porous SiO₂ film. It can be seen that the film dominantly consists of Si and O. The relative contents of Si and O are listed in table 2, which shows that the Si-to-O ratio of the porous film is nearly stoichiometric.

The Si2p and O1s XPS spectra of the porous SiO₂ are shown in figure 3. The Si2p and O1s peaks are centered at 103.35 eV and 532.65 eV, respectively. The binding energies

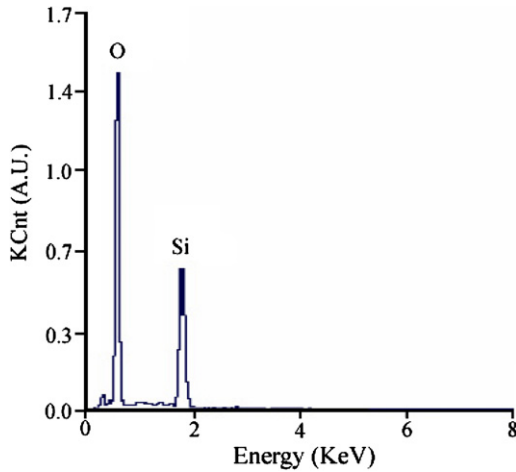
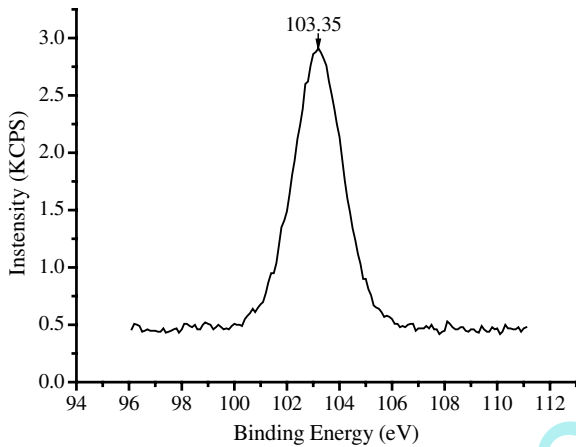
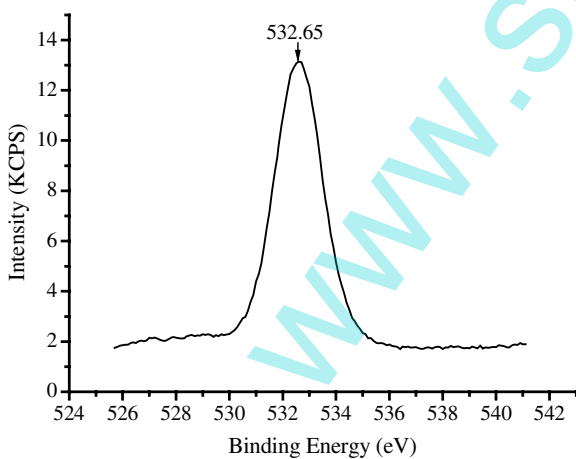


Figure 2. EDS spectra of the porous SiO₂ film.



(a)



(b)

Figure 3. XPS spectra of the porous SiO₂ film: (a) Si2p spectrum; (b) O1s peak.

at 103.35 eV for Si2p and 532.65 eV for O1s are assigned to O=Si=O. This indicates that Si and O in the film exist in SiO₂ form.

The porosity of a porous SiO₂ thin film can be assessed indirectly using refractive indices. According to the extended

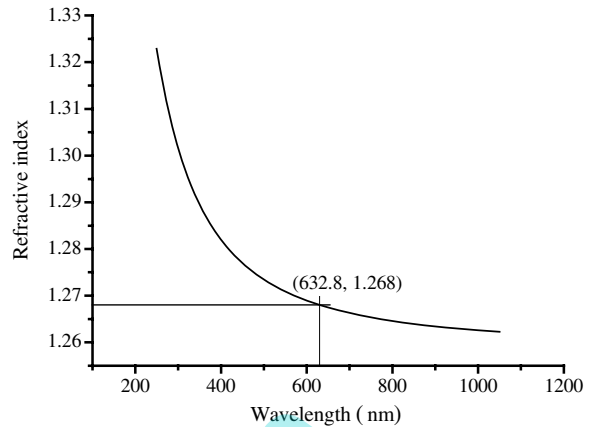


Figure 4. Refractive index of the porous SiO₂ film versus wavelength.

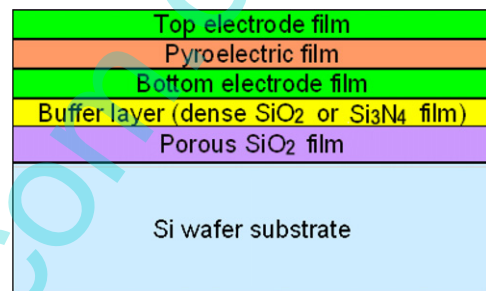


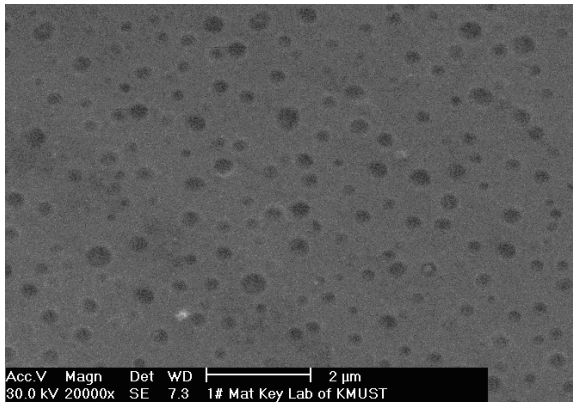
Figure 5. A schematic cross-sectional diagram of the multi-layer pyroelectric detector structure with a porous SiO₂ film.

Lorenta–Lorenz effective medium equation, the porosity, P , of a film can be obtained by [12]

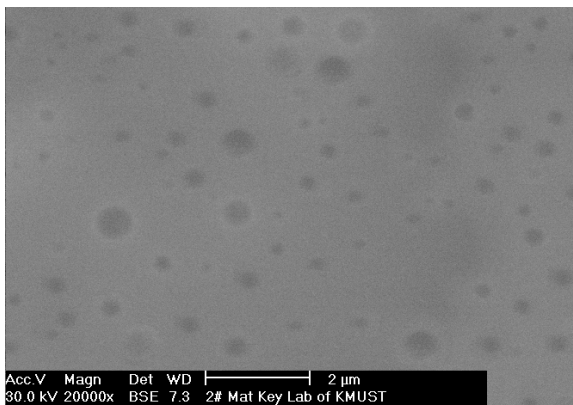
$$P = \frac{(n_{f0}^2 - n_b^2)(n_a^2 + 2n_b^2)}{(n_{f0}^2 + 2n_b^2)(n_a^2 - n_b^2)} \quad (1)$$

Here n_{f0} , n_b and n_a are the refractive indices of the porous SiO₂ film, the dense SiO₂ film and air (=1), respectively. Figure 4 provides the refractive index of the porous SiO₂ film versus the wavelength. At a 683.2 nm wavelength, the refractive index of the porous film is 1.268, while the refractive index of the dense film is 1.457. Based on equation (1), the calculated porosity of the porous SiO₂ film is 41.1%. Although the value is a little lower than that of porous SiO₂ films synthesized by the sol–gel technology [6], it may be enhanced by further optimization of deposition parameters.

A cross-sectional diagram of a simple multilayer pyroelectric detector with a porous SiO₂ film is shown in figure 5. The porous SiO₂ film acts as a thermal isolation layer to block the diffusion of heat flow from the pyroelectric film to the Si substrate. For practical applications, it is desirable to cap the porous film with a layer of dense SiO₂ or Si₃N₄ thin film which was also prepared by PECVD. To observe the pore structure, high-resolution SEM images of an as-deposited porous SiO₂ film and a sample capped with an ultrathin dense SiO₂ film were taken (figure 6). Figure 6(a) corresponds to the as-deposited porous SiO₂ sample, and it illustrates distinctly the pore structure of the SiO₂ film. Figure 6(b) shows the SEM image of the SiO₂ film sample with a capping layer of



(a)



(b)

Figure 6. SEM images of (a) the as-deposited porous SiO₂ film and (b) the porous SiO₂ film with a dense SiO₂ capping layer.

100 nm dense SiO₂ thin film. The pore structure can also be observed, though the number of the pores is decreased. In our study, the capping layer is 100 nm thick, and the porous SiO₂ thin film is 1350 nm thick. In comparison with the porous SiO₂ thin film, the capping layer is rather thin. So, it is reasonable to make a conclusion that most pores can be preserved after the deposition of the dense SiO₂ capping layer. In addition, comparing figures 6(a) and (b), we found that the surface of the porous SiO₂ thin film becomes much smooth after the deposition of the capping film. It is obvious that the capping film as a buffer layer is preferable to the growth of other functional thin films. Similarly, the porous SiO₂ film

as a thermal isolation layer can enhance the efficiency of a microbolometer which is another kind of uncooled infrared detector.

Conclusion

The porous SiO₂ film was deposited by optimized PECVD experimental parameters. Under the optimized process conditions, the film deposition rate was about 1 nm s⁻¹. The results of AFM, SEM and ellipsometer measurement show that the film has a loose porous structure with a porosity of 41.1%. Due to its good process compatibility with device fabrication, such a porous SiO₂ film can be conveniently used as thermal isolation layers of uncooled infrared detectors.

Acknowledgments

The authors would like to thank Professor Arne Roos (Uppsala University, Sweden) for his valuable help in polishing the English of this paper. Inspiring discussions with Dr Xiao-wen Zhang (Shanghai University, China) are gratefully acknowledged.

References

- [1] Rogalski A 2002 *Infrared Phys. Technol.* **43** 187–210
- [2] Hu M, Wu M, Lv Y, Dou Y and Cui M 2007 *Surf. Coat. Technol.* **201** 4858–60
- [3] Liu X, Han L and Liu L 2008 *IEEE Sens. J.* **8** 354–6
- [4] Liu W, Liu Y, Zhang L and Yao X 1995 *Infrared Phys. Technol.* **36** 865–8
- [5] Ruffner J A, Clem P G, Tuttle B A, Brinker C J, Sriram C S and Bullington J A 1998 *Thin Solid Films* **332** 356–61
- [6] Li L, Zhang L and Yao X 2004 *Ceram. Int.* **30** 1843–6
- [7] Jain A, Rogojevic S, Ponoth S, Agarwal N, Matthew I, Gill W N, Persans P, Tomozawa M, Plawsky J L and Simonyi E 2001 *Thin solid Films* **398** 513–22
- [8] Kitazawa N, Namba H, Aono M and Watanabe Y 2003 *J. Non-Cryst. Solids* **332** 199–206
- [9] Choy K L 2003 *Prog. Mater. Sci.* **48** 57–170
- [10] Borrás A, Barranco A and González-Elipe A R 2006 *J. Mater. Sci.* **41** 5220–6
- [11] Barranco A, Cotrino J, Yubero F, Espinós J P and González-Elipe A R 2004 *J. Vac. Sci. Technol. A* **22** 1275–84
- [12] Matsuda A, Matsuno Y, Tatsumisago M, Tsutomu M and Minami T 2001 *J. Sol-Gel Sci. Technol.* **20** 129–34